



Tomographic velocity model estimation with data-derived first and second traveltimes derivatives

Eric Duveneck, Tilman Klüver, and Jürgen Mann, Geophysical Institute, University of Karlsruhe

Copyright 2003, SBGf – Sociedade Brasileira de Geofísica

This paper was prepared for presentation at the 8th International Congress of The Brazilian Geophysical Society held in Rio de Janeiro, Brazil, September 14-18 2003.

Contents of this paper was reviewed by The Technical Committee of the 8th International Congress of The Brazilian Geophysical Society and does not necessarily represent any position of the SBGf, its officers or members. Electronic reproduction, or storage of any part of this paper for commercial purposes without the written consent of The Brazilian Geophysical Society is prohibited.

Summary

The Common-Reflection-Surface (CRS) Stack in its different variants can be used to extract kinematic information for the construction of velocity models from seismic prestack data. A tomographic inversion method is presented that makes use of this information, in the form of first and second spatial derivatives of traveltimes, to determine smooth, laterally inhomogeneous subsurface velocity models for depth imaging. The input for the inversion consists of picked CRS attributes at a number of locations in the simulated zero-offset (or common-offset) section obtained with the CRS Stack. During the iterative inversion process the required forward-modeled quantities are obtained by dynamic ray-tracing along central rays pertaining to the input data points. Fréchet derivatives for the tomographic matrix are calculated with ray perturbation theory. The inversion can be formulated for the 2-D and 3-D case with zero-offset central rays, as well as for the case of finite-offset central rays.

Introduction

The construction of velocity models is an important task for seismic depth imaging in laterally inhomogeneous media. An often used tool for the determination of velocity models is reflection tomography (e. g., Farra and Madariaga, 1988; Stork and Clayton, 1991). The drawback of tomographic methods, however, is the large amount of picking that is necessary to obtain traveltimes from the prestack data, often along continuous reflectors across the entire section. In a method introduced by Billette and Lambaré (1998), called Stereotomography, slope information of locally coherent events is used together with traveltimes to obtain a smooth model. With that approach, no interfaces need to be introduced in the model. Consequently, no picking along continuous events is necessary.

Recently, a tomographic method for the construction of smooth models based on the results of the Common-Reflection-Surface (CRS) Stack has been presented by Duveneck and Hubral (2002) and Duveneck (2003). This approach, which combines aspects of stacking-velocity-based inversion methods with concepts of Stereotomography, makes use of kinematic information in the form of wavefront curvatures and emergence angles extracted from the prestack data with the CRS Stack. Here, we will present an alternative formulation of this method, that is

especially well suited for an extension to the 3-D case. Instead of wavefront curvatures and emergence angles, it is formulated in terms of first and second spatial traveltimes derivatives. If the finite-offset variant of the CRS Stack is used, the kinematic information obtained with that method can also be applied in a tomographic inversion. The inversion with finite-offset CRS attributes then closely resembles Stereotomography, except that in addition to first derivatives, also second derivatives of the traveltimes are used.

CRS Stack and attributes

The CRS Stack (e. g., Jäger et al., 2001), which has originally been developed for obtaining simulated zero-offset (ZO) sections from seismic multicoverage data, is based on stacking operators that are of second order in the half-offset h and midpoint ξ coordinate. For each zero-offset sample to be simulated, optimum values for the coefficients of the stacking operator are found directly from the prestack data with a coherence analysis. Thus, these coefficients, which are by-products of the CRS Stack, contain kinematic wavefield information that can be used for the construction of velocity models for depth imaging.

For a given near-surface velocity value v_0 , the CRS operator coefficients can be described in terms of spatial domain wavefront attributes. In 2-D, these are two radii of wavefront curvature, denoted by R_{NIP} and R_N , and one emergence angle for each simulated ZO sample. Alternatively, apart from a description with ray propagator matrix elements and angles, a description directly in terms of time domain parameters (first and second spatial traveltimes derivatives) can be used, without the assumption of a near-surface velocity value (e. g., Schleicher et al., 1993). The respective quantities used to describe the CRS operator coefficients are called CRS attributes.

The CRS Stack has been extended to handle 3-D seismic data. In that case, the stacking operator is described by eight CRS attributes. For a given near-surface velocity value, these can be interpreted as two angles giving the emergence direction of the central (ZO) ray and three independent elements each, of two curvature matrices, called \underline{K}_{NIP} and \underline{K}_N . Again, an alternative description with two first and six second derivatives is possible.

In the finite-offset variant of the CRS Stack, second-order stacking operators are used, that locally approximate traveltimes around a given finite offset to obtain a simulated finite-offset (e. g., common-offset) section. The resulting five CRS attributes (2-D case) pertain to the associated finite-offset central ray. These CRS attributes can again be interpreted in terms of two emergence angles and three wavefront curvatures if near-surface velocity values are given, or, alternatively, in terms of two first and three second traveltimes derivatives.

Tomography with CRS attributes

Here, we will initially only consider the 2-D ZO case, i. e., CRS attributes obtained from the 2-D ZO CRS Stack. For the tomographic inversion presented here, the half travel-time $T = t/2$, its first derivative with respect to the midpoint coordinate, $p_\xi = \partial T / \partial \xi$, and its second derivative with respect to the half-offset, $M_h = \partial^2 T / \partial h^2$, all evaluated on the central (normal) ray, are used. It can be shown (e. g., Hubral, 1983), that up to second order in h , the CMP reflection traveltimes coincide with those of the corresponding NIP wave, i. e., the hypothetical wave that would be obtained from placing a point source at the normal-incidence point (NIP) of the ZO ray on the reflector. The quantity M_h , together with the one-way traveltime T along the normal ray, thus describes the approximate second-order traveltime of a NIP wave in the CMP configuration, while the quantity p_ξ contains information on the propagation direction of the NIP wave at the surface location ξ . All required quantities are directly obtained from the output of the CRS Stack.

The inversion is based on the criterion that in a correct velocity model all considered NIP waves, when propagated back into the earth along the normal ray, focus at zero traveltime. This is equivalent to the statement that in a correct model the CMP traveltimes (described by T and M_h), the emergence directions (given by p_ξ), and the emergence locations (ξ) of all considered NIP waves should be correctly modeled.

Forward modeling of the quantities p_ξ and M_h for a given ray starting location and initial slowness vector in the subsurface can be done by dynamic ray-tracing in global Cartesian coordinates with the depth coordinate z being the independent variable along the ray (e. g., Farra and Madariaga, 1987). The ray propagator matrix thus obtained is the surface-to-surface ray propagator matrix \mathbf{I} (e. g., Bortfeld, 1989), assuming horizontal posterior and anterior surfaces (turning rays are not considered here). As only a point source response (NIP wave) is considered, the assumption of a horizontal anterior surface in the subsurface does not imply any limitation to horizontal reflectors. The second horizontal derivative of the NIP wave traveltime, evaluated on the central ray, is then given by $M_h = DB^{-1}$, where D and B are elements of the ray propagator matrix \mathbf{I} . As the true ray starting locations and initial ray directions (local reflector dips) of the considered NIP waves are initially unknown, they have to be considered as part of the model to be inverted for, along with the velocity itself.

Formulation and solution of the inverse problem

In the 2-D case, the input for the tomographic inversion consists of a number of points picked in the CRS Stack and corresponding CRS attribute sections:

$$(T, M_h, p_\xi, \xi)_i, \quad i = 1 \dots n_{\text{data}}, \quad (1)$$

when n_{data} data points are used. Picked data points are independent of each other and do not have to follow events over consecutive traces. Each pick represents the entire approximate (second-order) multi-offset kinematic response of a NIP wave.

Each normal-incidence point (NIP) is characterized by its location in the subsurface (x, z) and the local horizontal

slowness component p_x of the normal ray, which also determines the local reflector dip. The smooth velocity model itself can be described by two-dimensional B-splines. Together with the reflection-point parameters, the B-spline coefficients v_{jk} define the model:

$$\begin{aligned} (x, z, p_x)_i & \quad i = 1 \dots n_{\text{data}}, \\ v_{jk} & \quad j = 1 \dots n_x, \quad k = 1 \dots n_z, \end{aligned} \quad (2)$$

where n_x and n_z are the chosen numbers of grid points in the horizontal and vertical directions. The inverse problem to be solved can be formally stated as follows: a model vector \mathbf{m} , consisting of the elements given in (2), is sought, that minimizes the misfit between a data vector \mathbf{d} , containing the picked values given in (1), and the corresponding modeled values $\mathbf{d}_{\text{mod}} = \mathbf{f}(\mathbf{m})$. The operator \mathbf{f} symbolizes the dynamic ray tracing in the given model. As a measure of misfit the least-squares norm (e. g., Tarantola, 1987) is used. The modeling operator \mathbf{f} is nonlinear, therefore a solution to the inverse problem is found in an iterative way by locally linearising \mathbf{f} and applying linear least-squares minimization during each iteration. For details on the solution strategy and regularization of the problem we refer to Duveneck and Hubral (2002) and Duveneck (2003). During each iteration, the Fréchet derivatives of \mathbf{f} at the current model, i. e., the quantities $\partial(T, M_h, p_\xi, \xi) / \partial(x, z, p_x, v)$, are required. These can be obtained during forward modeling with the help of ray perturbation theory, as described by Farra and Madariaga (1987).

Extension to the 3-D case

The formulation of the CRS Stack-based inversion presented here is well suited for an extension to the 3-D case. The inversion for a 3-D model is completely analogous to the 2-D case, but makes use of CRS attributes determined from the prestack data with the 3-D CRS Stack. The model can be described by velocity coefficients v_{jkl} and the parameters $(x, y, z, p_x, p_y)_i$ associated with the normal-incidence points in the subsurface, corresponding to the picked input data points (compare (2)). The choice of data components depends on the azimuth coverage available in the prestack data. If it is sufficient to allow a reliable determination of the entire matrix \mathbf{M}_h with the CRS Stack, this matrix can be used in the inversion. Theoretically, for each datapoint, only the second traveltime derivative in one specified azimuth direction \mathbf{n} , i. e., M_n , is required. Data are then given by $(T, M_n, p_{\xi_x}, p_{\xi_y}, \xi_x, \xi_y)_i$ (compare (1)).

Extension to the 2-D finite-offset case

The three wavefront curvature values (or alternatively three second derivatives of traveltime) obtained when applying the finite-offset CRS Stack depend not only on the velocity distribution in the subsurface, but also on the reflector curvature in the vicinity of the reflection point of the central ray. They can therefore not be directly used in an inversion without considering the local reflector curvature as an additional unknown. Bergler and Hubral (2003) have shown, however, that an approximation of the common-reflection-point (CRP) trajectory around the considered finite-offset sample in the prestack data space can be found from the CRS attributes. This allows to use the CRS attributes to calculate wavefront curvatures at the source and receiver side of a wave that focuses on the reflector at the reflection point of the central ray, thus eliminating the influence

of reflector curvature. The associated wavefronts can be reinterpreted as belonging to two hypothetical waves due to a point-source at the reflector, traveling upwards along the source and receiver ray, respectively. These are the finite-offset equivalents of the NIP wave discussed earlier. Instead of wavefront curvatures, again the associated second traveltimes derivatives M_s at the source location ξ_s and M_r at the receiver location ξ_r can be determined. These second traveltimes derivatives, together with the first traveltimes derivatives at the source and receiver side, p_{ξ_s} and p_{ξ_r} , the source and receiver coordinates themselves, and the traveltimes t along the finite-offset central ray can then be used in a tomographic inversion method similar to the one described above.

Data for the inversion thus consist of values $(t, M_s, M_r, p_{\xi_s}, p_{\xi_r}, \xi_s, \xi_r)_i$ picked and calculated from the finite-offset CRS Stack results. The model again consists of B-spline coefficients v_{jk} together with reflection point coordinates and, in this case, two horizontal slowness components (one for each ray segment) at the reflection point, $(x, z, p_s, p_r)_i$, associated with the picked input data. During the inversion, the quantities M_s and M_r and all other required quantities (for the calculation of Fréchet derivatives) can be computed independently along the two ray segments, which have coincident ray starting coordinates in the subsurface. Like the inversion based on 2-D ZO CRS attributes, the 2-D finite-offset inversion can alternatively be formulated in terms of wavefront curvatures and emergence angles.

The inversion approach based on common-offset CRS attributes closely resembles Stereotomography as introduced by Billette and Lambaré (1998), except that in addition, second derivative information M_s and M_r is used.

A synthetic data example

The synthetic example shown here has been obtained with the formulation of the inversion as presented by Duveneck (2003), i. e., data points $(T, M, \alpha, \xi)_i$ were used, where $M = 1/v_0 R_{\text{NIP}}$, v_0 is the near-surface velocity value used during the CRS Stack, and α is the normal ray emergence angle. The overall procedure is the same as described here, though. As a first step, the 2-D ZO CRS Stack was applied to the synthetic multicoverage data, modeled by ray-tracing in the blocky model displayed in Figure 1(c). 422 data points were then picked in the resulting simulated ZO section and associated CRS attribute sections. These served as the input for the inversion. The velocity model is defined by 18×14 B-spline coefficients on a grid with 500 m horizontal and 300 m vertical spacing. The start model was chosen to consist of a near-surface velocity of 2000 m/s and a vertical velocity gradient of 0.6 s^{-1} .

The inversion result after 8 iterations, consisting of the velocity model and the reconstructed normal rays, is displayed in Figures 1(a) and (b). The reconstructed model resembles a smoothed version of the true discontinuous velocity distribution. It is kinematically correct, i. e., local reflector elements (dip bars), attached to the end points of reconstructed normal rays, are, for the most part, placed in the correct subsurface positions. This is demonstrated in Fig. 1(c), where the reconstructed reflector elements are plotted into the original velocity model.

Conclusions

We have presented different variants of a tomographic method for the construction of smooth velocity models for depth imaging, based on first and second traveltimes derivatives. These can be extracted from seismic prestack data with the Common-Reflection-Surface Stack, applied either in its 2-D or 3-D zero-offset, or in its finite-offset version. Input data points for the inversion are picked from the CRS Stack section and the associated CRS attribute sections. Picks are independent of each other and do not have to follow events over successive traces across the section. While the inversion approach is similar to a previously presented method based on wavefront curvatures and emergence angles obtained with the CRS Stack, the formulation in terms of traveltimes derivatives considerably simplifies the application in the 3-D case.

Acknowledgments

We would like to thank the sponsors of the Wave Inversion Technology (WIT) Consortium for their support.

References

- Bergler, S., and Hubral, P., 2003, Finite-offset CRS attributes for imaging and inversion: SEG/EAGE Research Workshop, Expanded Abstracts.
- Billette, F., and Lambaré, G., 1998, Velocity macro-model estimation from seismic reflection data by stereotomography: *Geophys. J. Int.*, **135**, 671–690.
- Bortfeld, R., 1989, Geometrical ray theory: Rays and traveltimes in seismic systems (second-order approximation of the traveltimes): *Geophysics*, **54**, no. 3, 342–349.
- Duveneck, E., and Hubral, P., 2002, Tomographic velocity model inversion using kinematic wavefield attributes: 72nd Ann. Internat. Mtg., Soc. Expl. Geophys., Expanded Abstracts, 862–865.
- Duveneck, E., 2003, Determination of velocity models from data-derived wavefront attributes: 65th EAGE Conference and Exhibition, Expanded Abstracts.
- Farra, V., and Madariaga, R., 1987, Seismic waveform modeling in heterogeneous media by ray perturbation theory: *J. Geophys. Res.*, **92**, no. B3, 2697–2712.
- Farra, V., and Madariaga, R., 1988, Non-linear reflection tomography: *Geophys. J.*, **95**, 135–147.
- Hubral, P., 1983, Computing true amplitude reflections in a laterally inhomogeneous earth: *Geophysics*, **48**, no. 8, 1051–1062.
- Jäger, R., Mann, J., Höcht, G., and Hubral, P., 2001, Common-reflection-surface stack: Image and attributes: *Geophysics*, **66**, no. 1, 97–109.
- Schleicher, J., Tygel, M., and Hubral, P., 1993, Parabolic and hyperbolic paraxial two-point traveltimes in 3D media: *Geophys. Prosp.*, **41**, 495–513.
- Stork, C., and Clayton, R. W., 1991, Linear aspects of tomographic velocity analysis: *Geophysics*, **56**, no. 4, 483–495.
- Tarantola, A., 1987, Inverse problem theory: Methods for data fitting and model parameter estimation: Elsevier, Amsterdam.

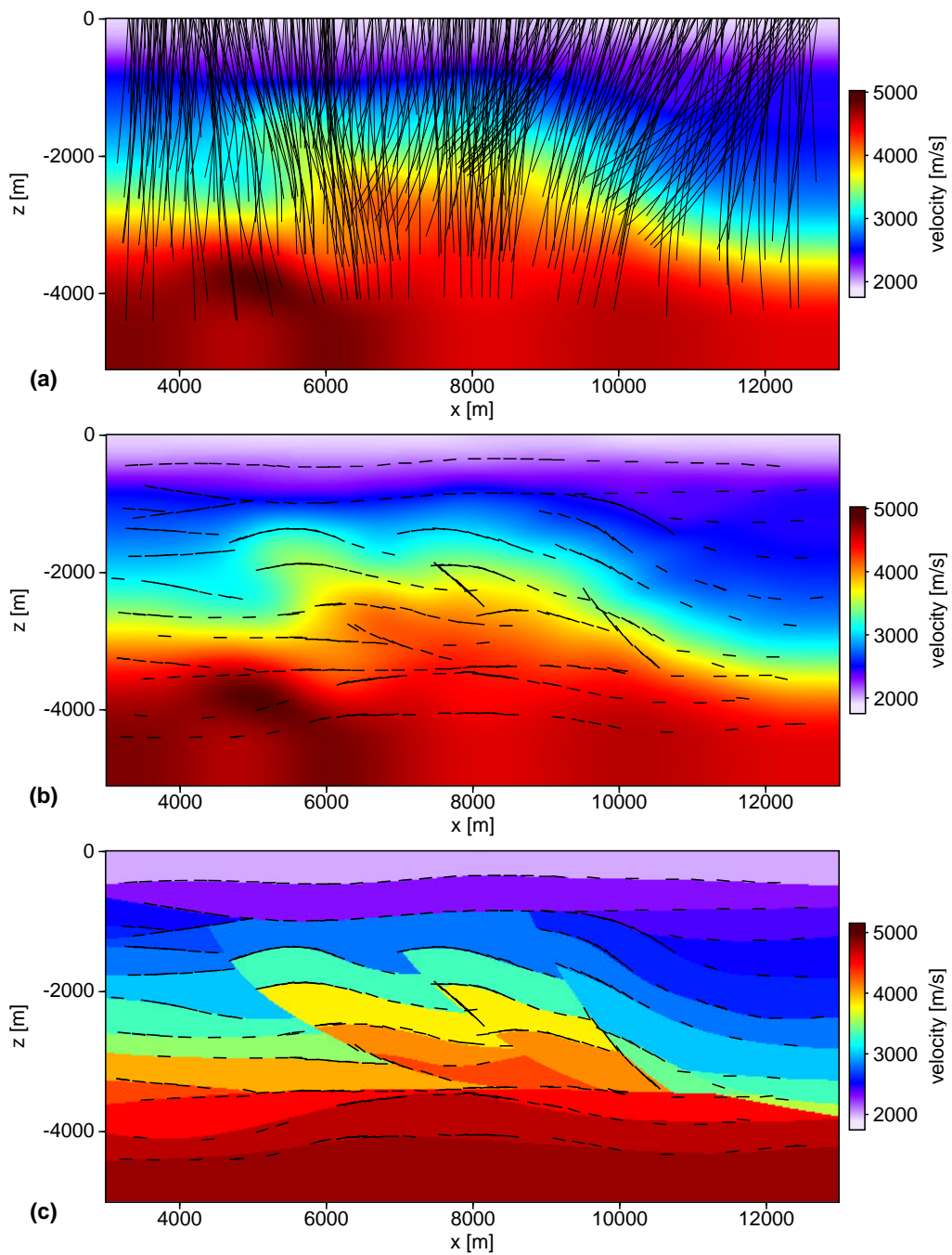


Figure 1: (a) Inversion result: reconstructed velocity model and normal rays. (b) Reconstructed model and reflector elements. (c) Reconstructed reflector elements superimposed onto the original blocky model. The prestack data were modeled by ray-tracing in the blocky velocity model. The input data for the inversion were picked from the CRS Stack and associated CRS attribute sections.